

Original Article

Two engineered site-specific antibody-drug conjugates, HLmD4 and HLvM4, have potent therapeutic activity in two DLL4-positive tumour xenograft models

Shijing Wang, Hui Wen, Wenyi Fei, Yuhong Zhao, Yuqi Feng, Lu Kuang, Min Wang, Min Wu

State Key Laboratory of Natural Medicines, School of Life Science and Technology, China Pharmaceutical University, Nanjing 210009, China

Received June 23, 2020; Accepted July 1, 2020; Epub August 1, 2020; Published August 15, 2020

Abstract: The humanized Delta-like 4 (DLL4) monoclonal antibody H3L2 with a quite high affinity for hrDLL4 inhibits the DLL4-mediated human umbilical vein endothelial cell (HUVEC) phenotype, inducing dysfunctional angiogenesis and tumour cell apoptosis, which effectively arrests breast cancer cell growth *in vivo*. To develop a more effective therapy, an engineered cysteine residue at alanine 121 (Kabat numbering) on each H3L2 heavy chain or at valine 207 (Kabat numbering) on each H3L2 light chain was established by site-directed mutagenesis. Three engineered antibodies, THL4, TH2 and TL2, were identified, and the specific-site antibody-drug conjugates (ADCs) THL4-mpeoDM1 (named HLmD4), TH2-mpeoDM1 (named HmD2), TL2-mpeoDM1 (named LmD2) and THL4-vcMMAE (named HLvM4), were produced, which exhibit much more potent antitumour activity than the naked antibody. The engineered ADCs can be directed against DLL4 and effectively internalized, followed by the release of small molecule cytotoxic agents, e.g., DM1 or MMAE, into the cytosol, which inhibit the synthesis of microtubules and induce G2/M phase growth arrest and cell death through the induction of apoptosis. ADC-conjugated DM1 was highly potent against DLL4-expressing cells *in vitro*. We systematically compared the *in vitro* potency and the *in vivo* preclinical efficacy and safety profiles of the heterogeneous conventional ADC, H3L2-mpeoDM1 (named JmD4) with that of the homogeneous engineered conjugate HLmD4. The engineered anti-DLL4 ADCs, particularly HLmD4, showed more potent antitumour activity than Docetaxel and superior safety compared with JmD4 in two xenograft tumour models. Our findings indicate that engineered ADCs have promising potential as effective preclinical therapies for cancers.

Keywords: DLL4, antibody-drug conjugates, specific-site, tumour models, DM1

Introduction

Delta-like 4 (DLL4) is a key Notch ligand in the Notch signalling pathway, which is dramatically confined to the vascular endothelium and highly expressed in tumour vasculature compared with normal tissues, as discovered in 2000 [1, 2]. DLL4/Notch inhibition is expected to have antitumour efficacy that has been demonstrated in preclinical models [3]. Many studies have reported that DLL4 is abnormally expressed in kinds of malignant tumours, including T-ALL leukaemia [4], breast cancer [5], pancreatic cancer [6] and lung carcinoma [7]. At present, a DLL4 fusion protein and anti-DLL4 monoclonal antibodies (mAbs) are being studied, and some antibody drugs are in phase II clinical trials by

the U.S. Food and Drug Administration (FDA), including REGN421 developed by Regeneron, which has been shown to inhibit solid tumour growth, especially in ovarian cancer [7]. However, the anti-DLL4 antibody OMP-21M18 was discontinued in a phase II clinical trial in 2017 because of a poor evaluation of survival, safety and pharmacokinetics [8].

Although targeted therapy using mAbs has revolutionized cancer treatment, antibodies against tumour-specific antigens have low activity or even lack therapeutic activity. Antibodies have been alternatively conjugated to a variety of cytotoxic drugs to obtain antibody-drug conjugates (ADCs), which reduce the systemic toxicity associated with traditional small-molecule

Engineered site-specific ADCs have potent therapeutic activity

chemotherapeutics and have more potent and promising therapeutic activity than naked antibodies. Currently, over 40 ADCs have entered clinical trials approved by FDA and European Medicines Accreditation Agency (EMA) [9], and 9 such drugs have been approved for sale: Mylotarg® [10], Adcetris® [11], Kadcyca® [12], Besponsa® [13], Lumoxiti® [14], Elzonris® [9, 15], Polivy® [16], Padcev® [17] and Enhertu® [18] (**Table 1**).

These ADCs are designed to directly target to its corresponding antigen localized on the cell, the entire ADC-antigen complex is internalized by receptor-mediated endocytosis and the cytotoxic drug is released into the cell, leading to cell death [19]. Therefore, ADCs firmly provide a significant increase in the therapeutic window compared with chemotherapy and radiation. However, the clinical development of ADC drugs requires careful development of many biological and pharmaceutical parameters, each of which requires careful optimization, such as antigen, linker, drug loading level and conjugation drug [20].

Selection of the linker, including its structure and chemistry, is a significant factor that contributes to the characteristics of ADCs, which is crucial for specificity, potency and safety [21]. A non-reducible bis-maleimido-trioxyethylene glycol (BMPEO) linker, which is highly stable in the bloodstream and not cleaved during the whole process, has been used to produce the mpeo-drug complex. Its ADC is hydrolysed into two parts, lysine-mpeo-drug and the antibody, occurring mainly in the lysosome leading to a lower risk of systemic toxicity [22]. Another highly stable peptide linker, valine-citrulline (vc), utilizes the differences in conditions between the bloodstream and the cytoplasm within tumour cells and is selectively cleaved by lysosomal enzymes, releasing the drug [23, 24]. Because of their superior stability and security, both linkers are of high recognition presently.

DM1, a derivative of maytansine, is a potent antimitotic inhibitor [25-27] and has been widely used in the research and development of ADCs, such as Kadcyca® which prolonged overall survival by half a year with an objective response rate of 44% [28]. MMAE is a synthetic analogue of the natural product dolastatin 10 that couples with vc to obtain vc-MMAE [29].

In the present study, we engineered reactive cysteine residues at specific sites in a novel anti-human DLL4 monoclonal antibody (H3L2) developed in our laboratory with the expected anti-angiogenic and antitumour effects [30], with proprietary intellectual property rights (No. ZL201510951483.8), to allow linker-drug complexes (mpeo-DM1 and vc-MMAE) to be coupled with defined stoichiometry and without disruption of the inter-chain disulphide bonds to produce the ADC drugs THL4-mpeoDM1 (named HLmD4), TH2-mpeoDM1 (named HmD2), TL2-mpeoDM1 (named LmD2) and THL4-vcMMAE (named HLvM4). These ADCs were evaluated in a series of experiments *in vitro* and *in vivo*. Compared with the DM1-conjugated anti-DLL4 ADC H3L2-mpeoDM1 (named JmD4), produced using a conventional chemical method, HLmD4 exhibited less liver toxicity and improved safety in mice in acute and short-term toxicity studies. In particular, the novel anti-DLL4 ADCs were found to have superior antitumour activities compared with the naked antibody H3L2. Furthermore, HLmD4 showed higher antitumour activity than HLvM4. Thus, the analysis of data from both the efficacy and safety studies demonstrates that HLmD4 may have therapeutic potential.

Materials and methods

Materials

The humanized anti-DLL4 antibody (H3L2) was previously developed in our laboratory [30]. HUVECs were obtained from the American Type Culture Collection (ATCC). HEK-293T cells and the eukaryotic expression vectors pMH3 and pCA-puro were preserved in our lab [29]. All cells were maintained and cultured as described [29, 30]. BALB/c nude mice and ICR mice were purchased from the Yangzhou University Comparative Medicine Centre, Yangzhou, China. All animals were treated following the standards of the Comparative Medicine Centre of Yangzhou University, and all animal experiments were carried out in accordance with the Animal of the Ministry of Health of the People's Republic of China (Document No. 55, 2001). This study was approved by Ethics committee of China pharmaceutical university.

Site directed mutagenesis, antibody expression and purification

We previously reported the construction and production of a humanized antibody targeting

Engineered site-specific ADCs have potent therapeutic activity

Table 1. Approved antibody-drug conjugates (ADCs)

| ADC | Target | Linker | Drug | DAR | Disease treated |
|-----------|----------|-------------------|------------------|-----|---|
| Mylotarg® | CD33 | AcBut-disulphide | Calicheamicin | 2-3 | Relapsed or refractory B-cell precursor acute lymphoblastic leukaemia (ALL) |
| Adcetris® | CD30 | Valine-citrulline | Auristatin | 4 | Hodgkin lymphoma, anaplastic large-cell lymphoma |
| Kadcyla® | HER2 | Valine-citrulline | DM1 | 3.5 | HER2-positive metastatic breast cancer |
| Besponsa® | CD22 | AcBut-disulphide | Calicheamicin | 4-7 | Acute lymphoblastic leukaemia (ALL) |
| Lumoxiti® | CD22 | N/A | Pseudotox | N/A | Hairy-cell leukaemia |
| Elzonris® | CD123 | N/A | Diphtheria toxin | N/A | Blastic plasmacytoid dendritic cell neoplasm (BPDCN) |
| Polivy® | CD79b | Valine-citrulline | Auristatin | 3.5 | Relapsed or refractory diffuse large B-cell lymphoma (DLBCL) |
| Padcev® | Nectin-4 | Valine-citrulline | Auristatin | 4 | Advanced urothelial carcinoma |
| Enhertu® | HER2 | Deruxtecan | DXd | 8 | HER2-positive metastatic breast cancer |

N/A = not applicable.

Engineered site-specific ADCs have potent therapeutic activity

DLL4, H3L2 [30]. Briefly, a cysteine residue was engineered at alanine 121 (Kabat numbering) of the heavy chain or at valine 207 (Kabat numbering) of the light chain of H3L2 to produce the mutant chains HC-A121C or LC-V207C, respectively (**Figure 1A, 1B**). The two chains were connected with the eukaryotic expression vectors pMH3 and pCA-puro, respectively, to obtain recombinant engineering plasmids, the nucleotide sequences of which were confirmed with sequencing by Genscript Corporation (Nanjing, Jiangsu, China). The three variants of antibody H3L2, named THL4, TL2 and TH2, were produced by transient expression in HEK293 cells from four plasmids at equimolar ratios (**Figure 1B**) and were purified by standard protein A affinity chromatography followed by ultrafiltration. The assembly of the reduced and non-reduced states of the three variants and H3L2 were observed by 12% SDS-PAGE analysis.

Engineering site-specific antibody conjugates

The method by which the linker BMPEO (Tokyo Chemical Industry, Japan) and the drug DM1 (Jiaheng Biotech, Shanghai, China) synthesized mpeo-DM1 was described by Jagath R [22]. Briefly, DM-1 was dissolved in dimethyl formaldehyde and was added dropwise to BMPEO dissolved in a solvent mixture containing dimethyl formaldehyde, acetonitrile and water (2:1:1) to react in an ice/water bath for 1 h. Then the mixture was brought to room temperature and purified by ultrafiltration. Before conjugation of the three mutant antibodies to DM1 derivatized with the maleimide-containing linker (mpeo-DM1), the blocking cysteine that was present on the introduced cysteine was removed by mild reduction at 25°C in PBS by the addition of a ten-fold molar excess of the reducing agent TCEP-HCl (Thermo Scientific, USA) followed by ultrafiltration. The three antibodies were incubated for 3 h at 25°C with dehydroascorbic acid (dhAA, Sigma-Aldrich) to reform the inter-chain disulphide bonds at a two-fold molar excess over the concentration of TCEP. The formation of inter-chain disulphide bonds was monitored by non-reducing SDS-PAGE. The mpeo-DM1 compound was incubated with the activated antibodies at 25°C for 1 h to produce three ADCs (HLmD4, LmD2 and HmD2), which were purified by ultrafiltration. The drug linker vc-MMAE (Chemicals, Shanghai, China) was

coupled to the variant THL4 to produce HLmM4 as a control. The JmD4 used in this study was prepared by randomly opening inter-chain disulphide bonds of the antibody to couple with drugs as described earlier [29].

Hydrophobic interaction chromatography (HIC)

The drug antibody ratio was determined under denaturing and reducing conditions by HIC using an Agilent 1200 HPLC system (Wilmington, DE, USA). Chromatographic separation was performed with mobile phase gradient elution on a TSK-GEL Butyl-NPR column (4.6×35 mm, particle size 2.5 mm; TOSOH; Tokyo, Japan). The elution conditions and detection methods were previously described [29].

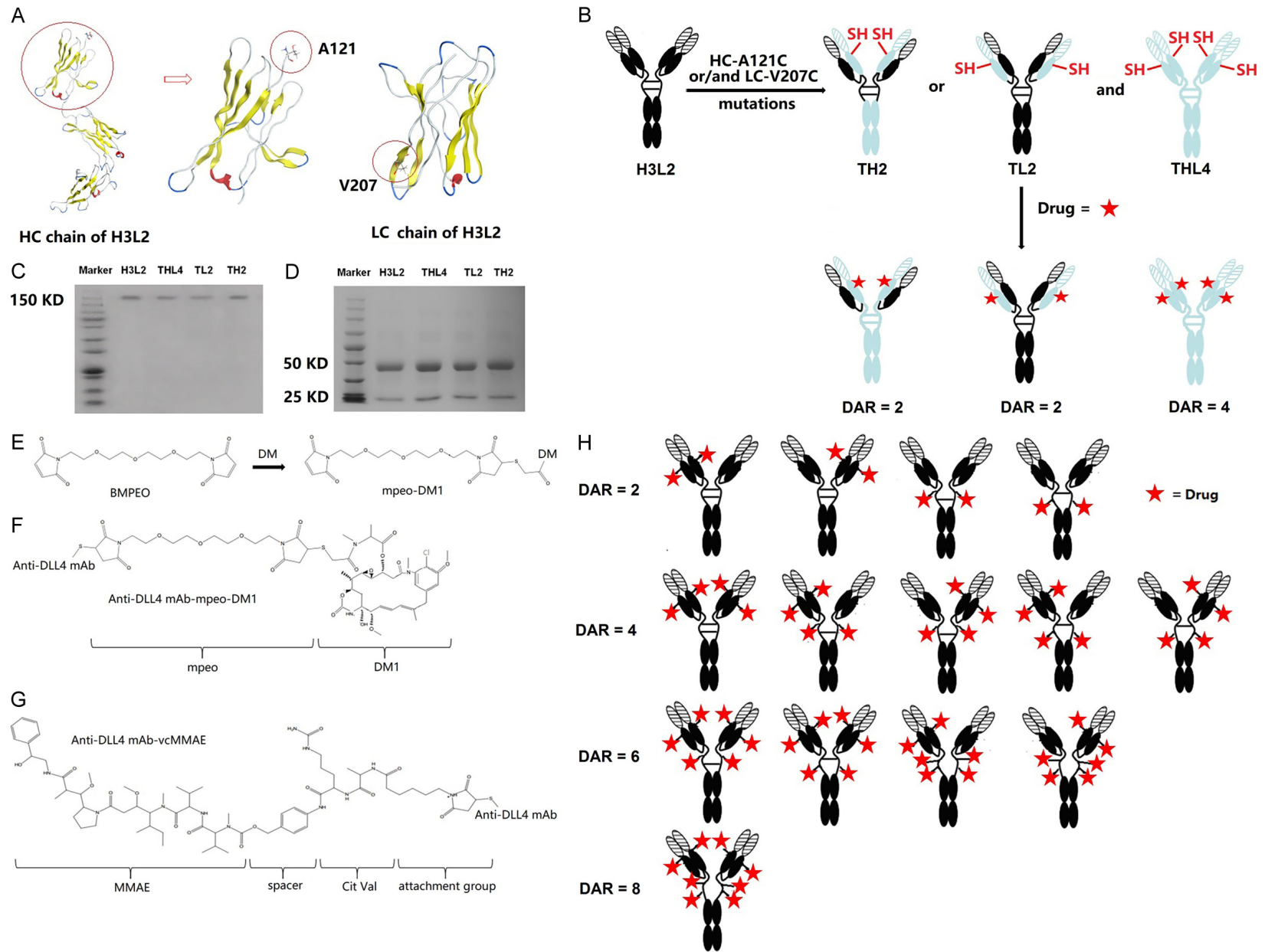
In vitro affinity, binding and internalization assays

ELISA was used to test the DLL4-binding capacity of the engineering site-specific ADCs. The procedures were previously reported in Xu et al. [31]. The absorbance of each well was measured using a plate reader at 450 nm and a reference of 630 nm.

HUVECs (4×10^5 cells per sample) were incubated on ice with drugs, followed by fluorescein isothiocyanate (FITC)-conjugated goat-antihuman IgG H+L (Sangon Biotech, Shanghai, China). The cells were analysed in detections one by one. A FACS flow cytometer (BD Biosciences, USA) was used to perform the binding assay, and the obtained data were processed using FlowJo 7.6 software.

To evaluate the internalization of the drugs *in vitro*, flow cytometry and confocal microscopy analyses were performed in HUVECs. The flow cytometry assay followed the procedures described above. The internalization percentage was calculated as (% internalization) = $[(MFI_{TimeX} - MFI_{background}) / (MFI_{Time0} - MFI_{background})] \times 100$ [32]. MFI is an abbreviated form of mean fluorescence intensity. A fluorescence microscope was used to directly observe the internalization effect. Drugs were labelled with the visible fluorescent dye rhodamine B (Beyotime Institute of Biotechnology, Shanghai, China) as described previously [29]. Observations were performed with a laser confocal microscope (Olympus FV1100).

Engineered site-specific ADCs have potent therapeutic activity



Engineered site-specific ADCs have potent therapeutic activity

Figure 1. Preparation of the three site-specific variants with engineered cysteine residues. (A) The three-dimensional molecular structure of the HC chain and LC chain in an antibody H3L2 and the rationale for conjugation site selection by the solvent accessibility, local charge and other factors. (B) The two sites (HC-A121C and LC-V207C) were selected to produce three variant antibodies (THL4, TL2 and TH2) in order to develop engineered site-specific anti-DLL4 ADCs conjugated with 2 or 4 drugs in the context of full-length antibody. The (C) non-reduced and (D) reduced 12% SDS-PAGE analysis of H3L2 and its variant antibodies (THL4, TL2 and TH2). (E) The equation to compound mpeo-DM1. BMPEO, a symmetric formula with two maleimide groups, was the same as vc conjugated via a maleimide group with the sulphhydryl group in the antibody. One of the two maleimide groups in BMPEO was attached to the sulphhydryl group in DM1, producing mpeo-DM1. (F) Molecular structure of ADC coupled with DM1. (G) Molecular structure of ADC coupled with MMAE. The complex contained a p-aminobenzyl carbamate spacer between vc and MMAE. (H) Illustration of conventional conjugate JmD4 with different drug load distributions. The ADC was prepared by controlled partial reduction of internal H3L2 disulfides with TCEP, followed by addition of the maleimide-mpeo-linker-DM1 with expected drug loads arising in intervals of 2, 4, 6 and 8 with related possible positional isomers.

In vitro plasma stability study

Blood samples (human) were purchased from Zhongda Hospital Affiliated with Southeastern University (Nanjing, China). The freshly extracted blood samples were collected and centrifuged. Drugs were added to the plasma samples at a final concentration of 100 µg/mL. Samples were transferred to a -80°C freezer at predetermined time points to stop the reaction. The collection at 0 h was put on dry ice within the first minute after drug addition. Samples were stored at -80°C until further analysis. Flow cytometry was used to determine the mean fluorescence intensity. The calculation and analysis methods were as described above.

Cell killing ability assay, induction of apoptosis of ADCs and evaluation of ADCs in the cell cycle in vitro

The MTT method was used for the cell killing ability assays in the presence of drugs for 48 h, and was carried out in HUVECs in a 96-well format as described previously [29].

We used flow cytometry to detect the induction of apoptosis by ADCs and evaluate the ADCs in the cell cycle. Cells (3×10^5) were incubated with different drugs. For the apoptosis evaluation, each cell sample was stained with annexin V-FITC and propidium iodide (PI) from an apoptosis detection kit (Sangon Biotech, China). The percent apoptotic cells was calculated as the sum of the percentages of early apoptotic cells and late apoptotic cells. For the cell cycle evaluation, each cell sample was stained with PI solution (Beyotime Biotech, China). The cell populations at different phases were quantified using ModFit analysis software.

To further confirm apoptosis induced by ADCs, we used a Caspase 3/7 Activity Kit (Beyotime Biotech, China) to detect the levels of caspase 3/7 (key enzymes in cell apoptosis). The absorbance of each sample was measured at 405 nm. The caspase 3 activity in each sample was calculated according to the standard curve constructed from the standard assay.

Western blotting for α/β -tubulin

To explore how small-molecule drugs block DNA synthesis by targeting tubulin, we used Western blotting to detect α/β -tubulin expression. Cells (1×10^6) were incubated with drugs for 24 h and then centrifuged and collected, followed by the addition of 100 µL of IP Cell Lysis solution (Beyotime Biotech, China) with 1 mM PMSF. Then the procedures for Western blotting were previously reported in Jia et al. [30].

ADC in vivo efficacy, stability and safety studies

Human breast adenocarcinoma (MDA-MB-231) and human non-small cell lung cancer (A549) xenograft BALB/c nude mouse models were established by Keygene Biotech, China. The mice were randomly assigned into treatment groups (6 mice/group) with an average tumour volume of 100 mm³/group. Drugs were intravenously (i.v.) administered in total three times on days 1, 4 and 7. H3L2 was intravenously administered once every three days for three weeks. The weights of the mice and the tumour size were recorded once every three days. The tumour volumes were determined according to the following formula: (length \times width²)/2.

BALB/c nude mice (n = 6/group) were administered ADCs (5 mg/kg) i.v. Blood samples were collected by orbital sampling once every two

Engineered site-specific ADCs have potent therapeutic activity

days for 28 days following dosing. Blood samples were processed to obtain plasma and then stored at -80°C until analysis to test the stability. The following treatments by FCS were the same as describe above.

The safety profiles for the ADCs were evaluated in ICR mice assigned to eight groups ($n = 6/\text{group}$). After administration, blood was collected for haematology and serum chemistry analysis. The platelet count was observed under a microscope, and the level of aspartate aminotransferase was analysed using an AST detection kit (Nanjing Jiancheng Bioengineering Institute, China).

Immunohistochemistry and immunofluorescence

After administration, the mice were dissected on the 21st day. The treatment method of the samples for immunohistochemistry (IHC) and immunofluorescence (IF) staining were described previously in Xu et al. [31]. All images were obtained under a fluorescence microscope.

Statistical analysis

The data are presented as the means \pm standard deviations (SD). Statistical analyses were performed using Student's t-test, and P values of 0.05 or less were considered statistically significant. Calculations were performed using GraphPad Prism software (GraphPad Software Inc., La Jolla, CA, USA).

Results

Preparation of the site-specific conjugates with engineered cysteine residues

Jagath R, Junutula used a series of experiments to research engineered cysteines at three sites, differing in solvent accessibility, local charge and other factors, to make comparisons to assess the impact of the conjugation site [31]. Applying this approach to the anti-DLL4 humanized antibody H3L2 suggested suitability of the variants LC-V207C and HC-A121C (Kabat numbering) for the site-specific labelling of the light and heavy chains, respectively, we decided to select these two sites to develop conjugates in the context of the full-length antibody (**Figure 1A**). Three groups of different engineered plas-

mids (four per group) were assembled in the eukaryotic expression system, to obtain three mutant antibodies (THL4, TL2 and TH2) (**Figure 1B**). After purification, the 12% SDS-PAGE analysis showed that H3L2, THL4, TL2 and TH2 contain heavy and light chain bands with clear molecular weights of approximately 25 and 50 kDa, respectively (**Figure 1C, 1D**).

Then, we explored the conjugation of anti-DLL4 antibodies with two linkers (BMPEO and vc) and two cytotoxins (DM1 and MMAE), producing mpeo-DM1 (**Figure 1E**) and vc-MMAE. Both cytotoxins inhibited the polymerization of tubulin in dividing cells. The resultant ADCs were used in these studies and are shown in **Figure 1F, 1G**. Since H3L2, as well as THL4, TH2 and TL2, is an anti-DLL4 IgG1 antibody, each antibody molecule contains four inter-chain disulphide bonds. The reduction of all disulphide bonds generates free sulphhydryl groups, and the oxidation of these sulphhydryl groups generates interchain disulphide bonds, only permitting the conjunction at specific-site residues using maleimide-containing linkers to produce conjugate compounds at a limited number of defined sites. Therefore, we obtained four anti-DLL4 ADCs, THL4-mpeoDM1 (named HLmD4), TH2-mpeoDM1 (named HmD2), TL2-mpeoDM1 (named LmD2) and THL4-vcMMAE (named HLvM4). The HIC analysis showed a uniform drug antibody ratio (DAR) distribution with 2-DAR (HmD2 and LmD2) or 4-DAR (HLmD4 and HLvM4) species, and more than 90% of the drugs were attached to single conjugation sites via the engineered cysteine residues (**Figure 2A**). According to the percent peak proportion of the HIC, the ratio of the peak of HmD2 or LmD2 with 2-DAR species was approximately 90% or 89.6% respectively and the average DAR was 2.32 or 2.4. The HLmD4 and HLvM4 had about 92.8% and 90.2% 4-DAR species with an average DAR of 3.96 and 3.92, respectively.

We previously reported that a murine anti-DLL4 ADC MMGZ01-vc-MMAE (MvM03) prepared by the conventional method displays higher antitumour activity than the naked antibody, although MvM03 contained a heterogeneous mixture of a variety of DAR complexes with MMAE conjugated to different light chain and heavy chain cysteine residues generated from inter-chain disulphide bonds reduced by tris (2-carboxy-

Engineered site-specific ADCs have potent therapeutic activity

ethyl) phosphine hydrochloride (TCEP) [29]. To examine whether the engineered HLmD4 conjugate would show certain homogeneity in drug conjugation, we used the above traditional method to couple mpeo-DM1 to cysteine residues on humanized H3L2 without mutation to generate H3L2-mpeoDM1 (named JmD4) as a control. Then, we analysed the DAR distribution for both the conventional and engineered conjugates by HIC analysis (**Figure 2A**), which allowed for the resolution of JmD4 into five major peaks corresponding to zero, two, four, six, and eight drug molecules per antibody with a DAR of 4.39, as shown in **Figure 1H**. Although HLmD4 and JmD4 were similar in terms of DAR, the former had greater homogeneity than the latter. Hence, in the following studies, we focused on HLmD4, JmD4 and HLvM4 to research their biological activity *in vitro* and antitumour activity and safety *in vivo*.

Binding ability, affinity, internalization, and plasma stability assays of H3L2 and ADCs in vitro

We tested these conjugates for their ability to bind to DLL4-expressing Human umbilical vein endothelial cells (HUVECs) using flow cytometry analysis, which showed certain binding signals of ADCs and H3L2 in HUVECs, compared with the DLL4-negative cell line HEK-293T (**Figure 2B**). These conjugates were able to bind to these cells in a manner similar to that of the unconjugated antibody H3L2 (**Figure 2C**). The enzyme-linked immunosorbent assay (ELISA)-based binding assay revealed the dose-dependent binding profiles of the ADCs to immobilized hrDLL4, and the three ADCs showed high affinities slightly lower than that of H3L2 (**Figure 2D**). In addition, engineered ADCs and traditional ADCs, similar to H3L2, can be efficiently internalized in HUVECs through endocytosis (**Figure 2E-G**). In the *in vitro* plasma stability study, the ADCs showed a similar stability trend with H3L2 for 144 h (**Figure 2H**).

Evaluation and analysis of cell killing and microtubulin levels by ADCs in vitro

The cytotoxicity of ADCs was assessed by MTT assay after 48 h of continuous exposure to H3L2, anti-DLL4 ADCs, Docetaxel and DM1 (1280, 640, 320, 160, 80, 40, 20, 10, 5, and 1 nM). The ADCs coupled with DM1 had similar cytotoxicities, with a median inhibitory concen-

tration (IC₅₀) < 50 ng antibody/mL against HUVECs. They exhibited an enhanced cell killing ability compared to that of the ADCs coupled with MMAE and Docetaxel (a marketed microtubulin inhibitor) and significantly inhibited the growth of cells in comparison to H3L2 (**Figure 3A**). Moreover, studies have found that the aggregation of α -tubulin and β -tubulin were inhibited by DM1 and MMAE. In contrast, Docetaxel promoted the aggregation of α -tubulin and β -tubulin to form tubulin polymers [33, 34]. Thus, proteins were extracted from the cells with treatments and the effects of the drugs on the levels of α -tubulin and β -tubulin in HUVECs was analysed by Western blot. As expected, the ADCs showed the same result as DM1 and MMAE was able to promote the aggregation of α -tubulin and β -tubulin, and the Docetaxel group had the opposite result compared to the above groups (**Figure 3C**).

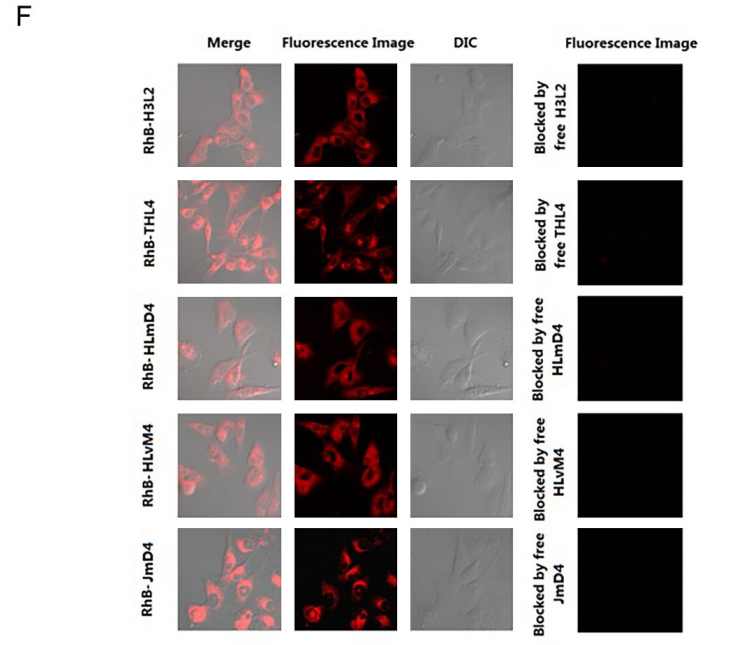
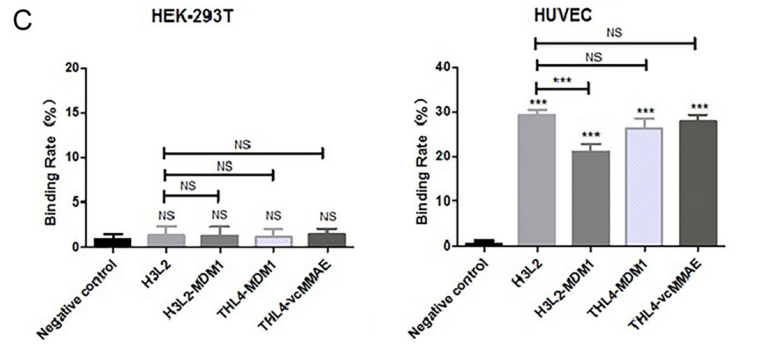
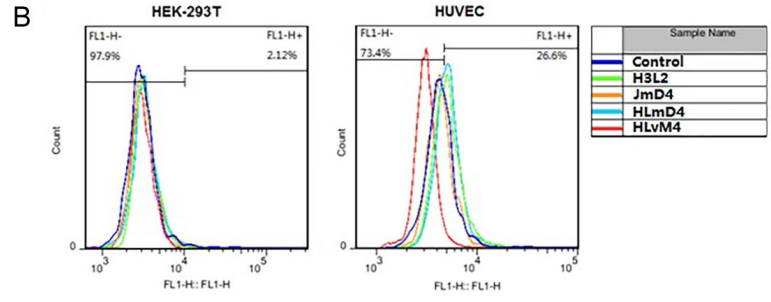
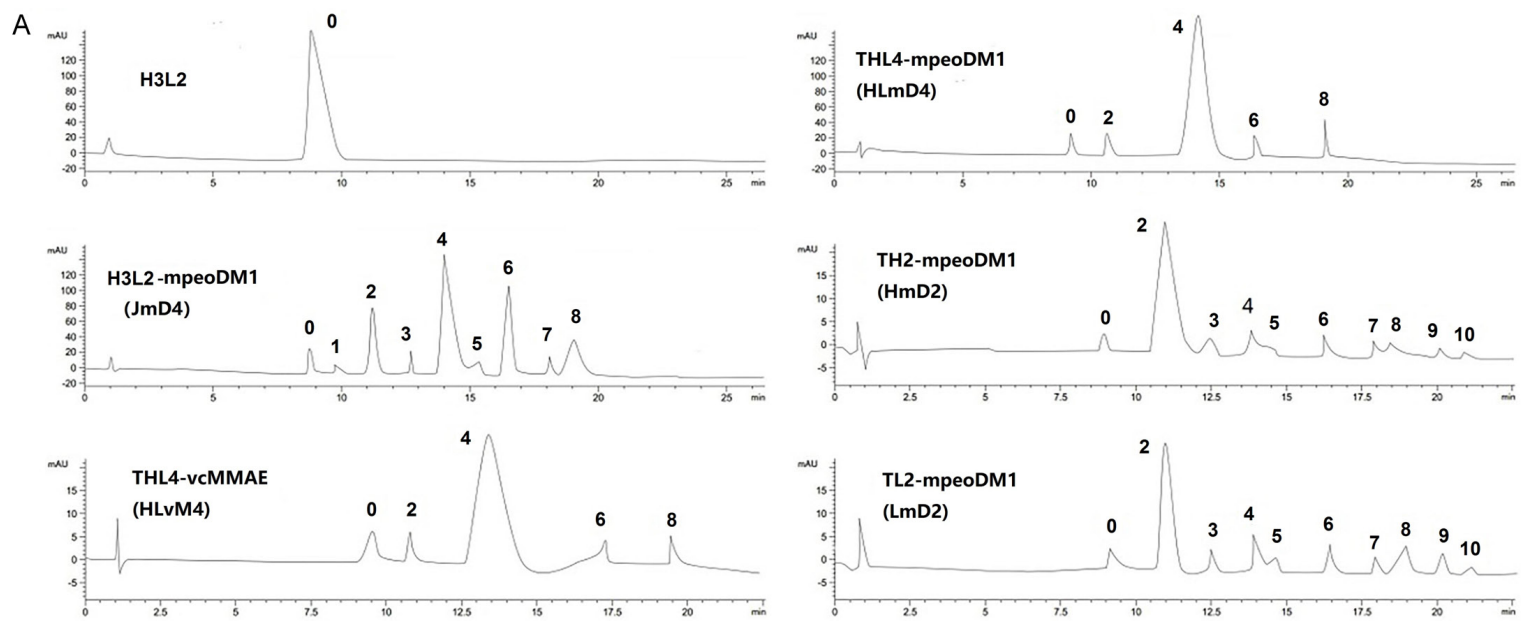
Assay of cell apoptosis and alterations in the cell cycle caused by ADCs in vitro

To further determine whether after treatment with the three ADCs the inhibitory effect on proliferation was associated with cell apoptosis and alterations in the cell cycle, HUVECs were examined by flow cytometry following treatment with ADCs and controls for 24 h. These ADCs, especially HLmD4 and JmD4, led to enhanced tumour cell apoptosis. The apoptosis rates of DM1, Docetaxel, HLmD4, HLvM4 and JmD4 were 63.3%, 66.39%, 56.2% and 59.36%, respectively (**Figure 3D**). Furthermore, these ADCs increased caspase 3/7 activity (**Figure 3B**). However, compared with Docetaxel and DM1, the cell apoptosis rates and caspase 3/7 activity in the ADCs coupled with DM1 were lower (**Figure 3D, 3E**). On the other hand, tubulin is involved in the G2 phase of the cell growth cycle [35]. Cell cycle analysis suggested that the cells in G2/M phase were increased, and those in the G0/G1 phase were decreased after the ADCs conjugated DM1 or MMAE treatment, and demonstrated that HLmD4, HLvM4 and JmD4 can arrest the cells in the G2/M phase (**Figure 3F, 3G**).

Comparison of the effects of ADC treatment on tumour growth, angiogenesis, proliferation, and apoptosis in vivo

To evaluate the efficacy of ADCs targeting hrDLL4 in breast tumours or non-small cell lung

Engineered site-specific ADCs have potent therapeutic activity



Engineered site-specific ADCs have potent therapeutic activity

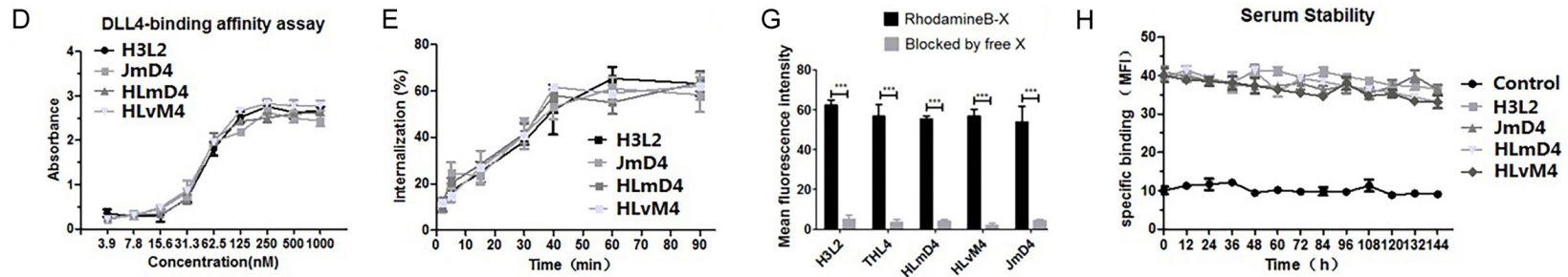


Figure 2. Characterization of antibody-drug conjugates. A. Hydrophobic interaction chromatography (HIC) analysis of ADCs. The site-specific ADCs on a butyl-NPR column yielded a predominant peak corresponding to naked antibody including two or four drug molecules. B, C. The binding rates of H3L2, HLmD4, JmD4 and HLvM4 in HUVECs were 29.33%, 26.37%, 21.11% and 27.77%, respectively, while those in DLL4-negative HEK-293T were 1.25%, 1.08%, 1.20% and 1.39%, respectively. D. hrDLL4-binding test for the affinity of ADCs (EC50 values of H3L2, HLmD4, HLvM4 and JmD4 were 49.22 nM, 42.57 nM, 40.7 nM and 37.68 nM, respectively). E. ADCs targeting DLL4 rapidly internalized into HUVEC cell within 40 min. The internalization rates were stabilizing at about 85 min. F. Laser confocal fluorescence microscopy images of HUVEC cells incubated with the RhB-ADCs, RhB-H3L2 and RhB-THL4 fluorescent probe, with or without a blocking dose of free these drugs. G. Mean fluorescence intensity of HUVEC cells treated with RhB-ADCs probes, compared with blocking with free ADCs. H. The plasma stability of ADCs is dependent on the antibody, especially variable region due to guarantee the effective endocytosis. Samples at predetermined time points (0, 12, 24, 36, 48, 60, 72, 84, 96, 108, 120, 132 and 144 h) were test by Flow cytometry. The ADCs showed a similar trend on stability with H3L2 for 144 h. Data were given as the mean \pm SD (n = 3). ***P < 0.001. NS: no significance.

Engineered site-specific ADCs have potent therapeutic activity

cancer, BALB/c nude mice were xenografted with MDA-MB-231 or A549 tumours. Compared with the vehicle control group, the inhibitory rates of MDA-MB-231 tumour growth in animals treated with 5 mg/kg Docetaxel, 5 mg/kg H3L2, 5 mg/kg HLmD4, 1.5 mg/kg HLmD4, 5 mg/kg HLvM4, 5 mg/kg JmD4 and DM1 of corresponding concentration were 32.88%, 47.86%, 86.11%, 57.73%, 82.33 %, 88.43% and 94.89 %, respectively. In the A549 model, the treatment of mice with 5 mg/kg of H3L2 resulted in a 21.14% decrease in the tumour volume compared with the treatment with normal saline, and the treatment with 5 mg/kg of Docetaxel resulted in a 37.92% decrease; the treatment with DM1, 5 mg/kg HLmD4, (1.5 mg/kg HLmD4), 5 mg/kg HLvM4 and 5 mg/kg HLvM4 resulted in a 90.33%, 80.25% (51.61%), 73.19% and 84.38% inhibition, respectively. The results showed that the high dose (5 mg/kg) groups, especially the ADCs coupled with DM1 groups, induced significant and durable tumour regression in both models. In contrast, the H3L2 and Docetaxel treatments only caused a slight delay in tumour growth. The same antitumour activity was observed in the A549 tumour xenografts. Of the three ADCs, HLmD4 and JmD4 showed optimal inhibition of tumour growth (**Figure 4A, 4B**).

Immunohistochemistry (IHC) staining tested the effects of the ADCs targeting hrDLL4 on Ki67 (a mitotic index) and cleaved caspase 3 (an apoptotic index) in MDA-MB-231 or A549 tumours (**Figure 4C-F**). After treatment with ADCs, a pronounced reduction in Ki67 levels and an increase in cleaved caspase 3 were observed in both tumours. Moreover, treatment with ADCs lead to a more evident reduction in Ki67 in tumour growth compared with that after H3L2 or Docetaxel treatments. Then to detect apoptosis, tumour sections stained for cleaved caspase 3 revealed that ADC treatment resulted in much higher levels of cleaved caspase 3 than H3L2 or Docetaxel treatment. In addition, in both tumour tissues, the ADCs coupled with DM1 treatment led to a greater decrease in the expression of Ki-67 and a greater increase in cleaved caspase 3 compared with the treatment with ADC coupled to MMAE (**Figure 4G, 4H**).

Furthermore, as measured using a CD31 antibody and an α -smooth muscle actin antibody

after treatment with ADCs, the percent of smooth muscle actin (SMA)-positive mural cells decreased in both tumour tissues. In particular, the tumours treated with ADCs coupled with DM1 were identified as similar to the negative control compared with ADC coupled with MMAE. The group treated with DM1 as a positive control revealed considerable toxicity. Moreover, compared with the A549 tumour tissues treated with ADCs, the MDA-MB-231 tumour tissues treated similarly showed a significant effect, which is lined with the results of the IHC analysis (**Figure 5**).

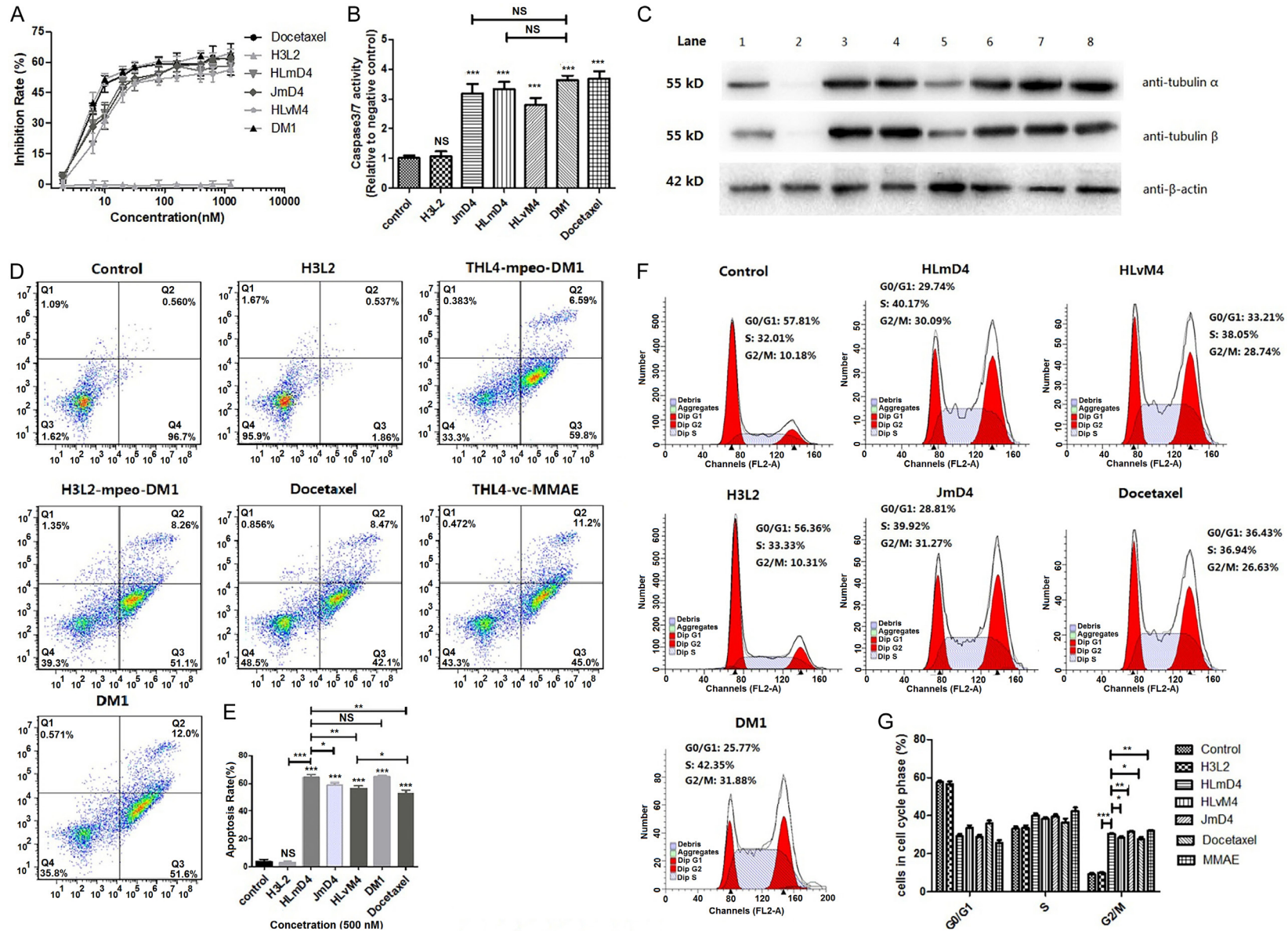
These results suggest that ADCs, especially ADC-conjugated DM1, inhibited tumour cell proliferation and induced apoptosis in tumour tissues.

Stability and safety assays of ADCs in vivo

Since the toxicities of DM1 conjugates are similar to those of DM1 and are not directly related to the binding antigen, we chose mice as an appropriate safety model regardless of affinity differences for DLL4 binding. The anti-DLL4 ADCs from the serum of BALB/c nude mice bound to human DLL4 in HUVECs with similar affinity, albeit with slightly lower affinity than that of the naked antibody (**Figure 6A**). To determine whether an engineered ADC format would improve the tolerability of the DM1 conjugates, we compared the safety profiles of the THL4 conjugates and H3L2 conjugates in ICR mice. After treatment with conventional ADC, DM1, MMAE and Docetaxel, there was a elevation in serum aspartate aminotransferase (**Figure 6B**) and reduced platelet counts (**Figure 6C**) observed at 6 days postdose than those of the engineered ADCs, and all drugs returned to levels comparable with those of the vehicle control mice by study day 12. Although the differences in these increases and decreases between groups were small, other safety test results revealed that engineered ADC had greater safety than conventional ADC.

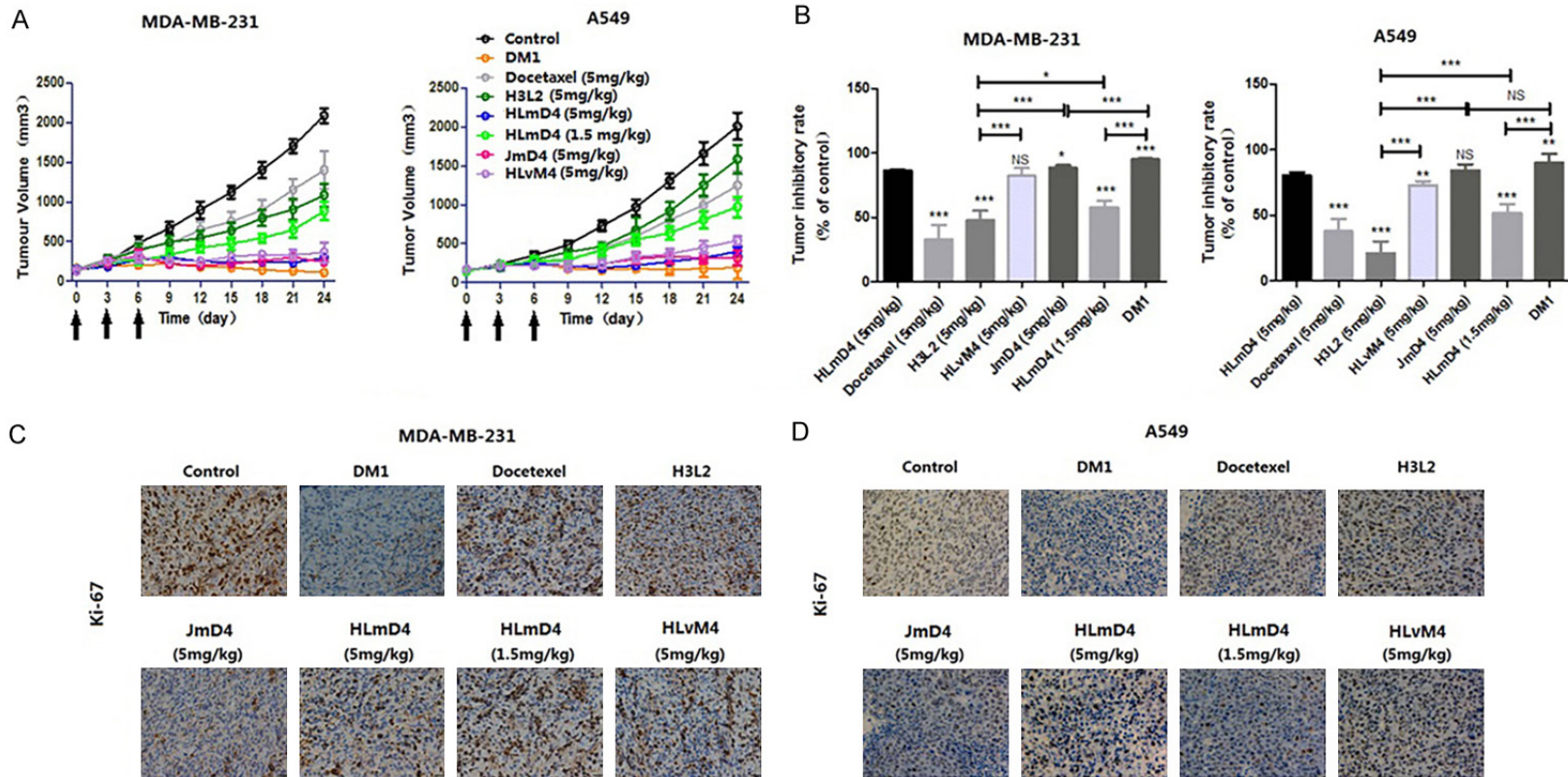
The results of the observed weights of the mice in both models, especially the MDA-MB-231 model, showed that engineered ADCs were generally well tolerated and maintained a nearly constant body weight, unlike the other compounds, which resulted in weight loss or gain. In particular, the DM1 and JmD4 treatment groups lost more weight, which demonstrated

Engineered site-specific ADCs have potent therapeutic activity



Engineered site-specific ADCs have potent therapeutic activity

Figure 3. *In vitro* cytotoxicity and mechanism of anti-DLL4 ADCs. A. The cytotoxicity of ADCs was assessed by MTT assay. The percentage of cell inhibition relative to untreated control HUVEC cells was calculated for each drug concentration. The three ADCs, especially the conjugates with DM1, induced potent anti-proliferative effects in HUVEC. The IC50 value of Docetaxel, HLmD4, JmD4, HLvM4 and DM1 was 10.57 nM, 37.45 nM, 36.12 nM, 40.53 nM and 11.72 nM, respectively. B. ADCs for 24 h examined by caspase 3/7 activity. C. Western blotting for α -tubulin and β -tubulin. ADCs conjugated with DM1 or MMAE inhibit the formation of α & β -tubulin dimmer. Lane 1: Negative control; Lane 2: Docetaxel; Lane 3: DM1; Lane 4: MMAE; Lane 5: H3L2; Lane 6: HLmD4; Lane 7: HLvM4; and Lane 8: JmD4. D. ADCs induce apoptosis of HUVEC cell. The cells were separately treated with corresponding concentrations of Docetaxel, DM1, H3L2 analyzed by flow cytometry following staining with Annexin V-FITC and PI. E. Quantitative analysis of apoptosis assay. F. Cell cycle analyzes HUVEC cells which were incubated with certain concentrations of drugs for 24 h and stained with PI. The percentage of cells in each phase was indicated. G. Quantitative analysis of cell cycle assay. Data were presented as the mean \pm SD, n = 3, *P < 0.05, **P < 0.001, ***P < 0.005. NS: no significance.



Engineered site-specific ADCs have potent therapeutic activity

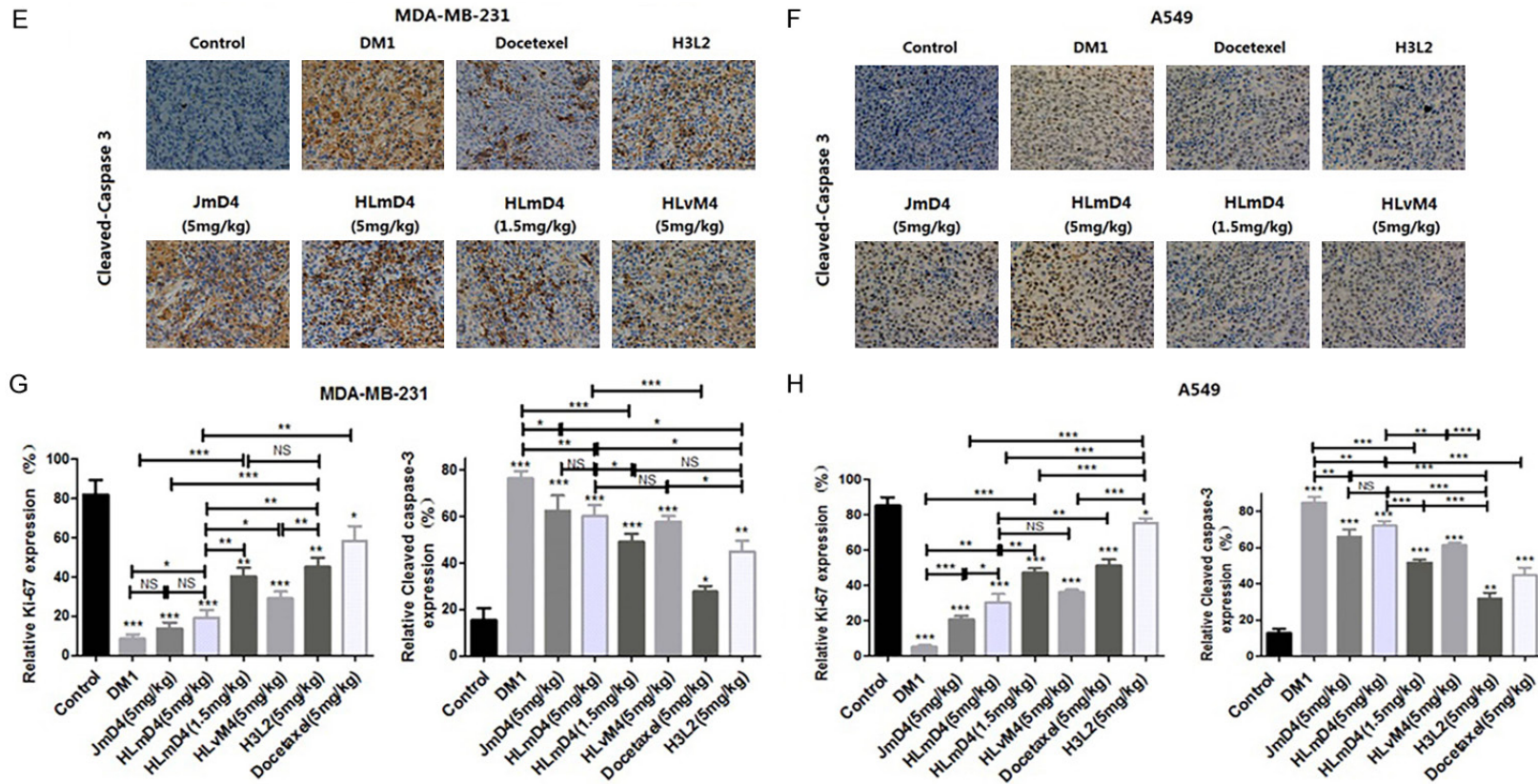
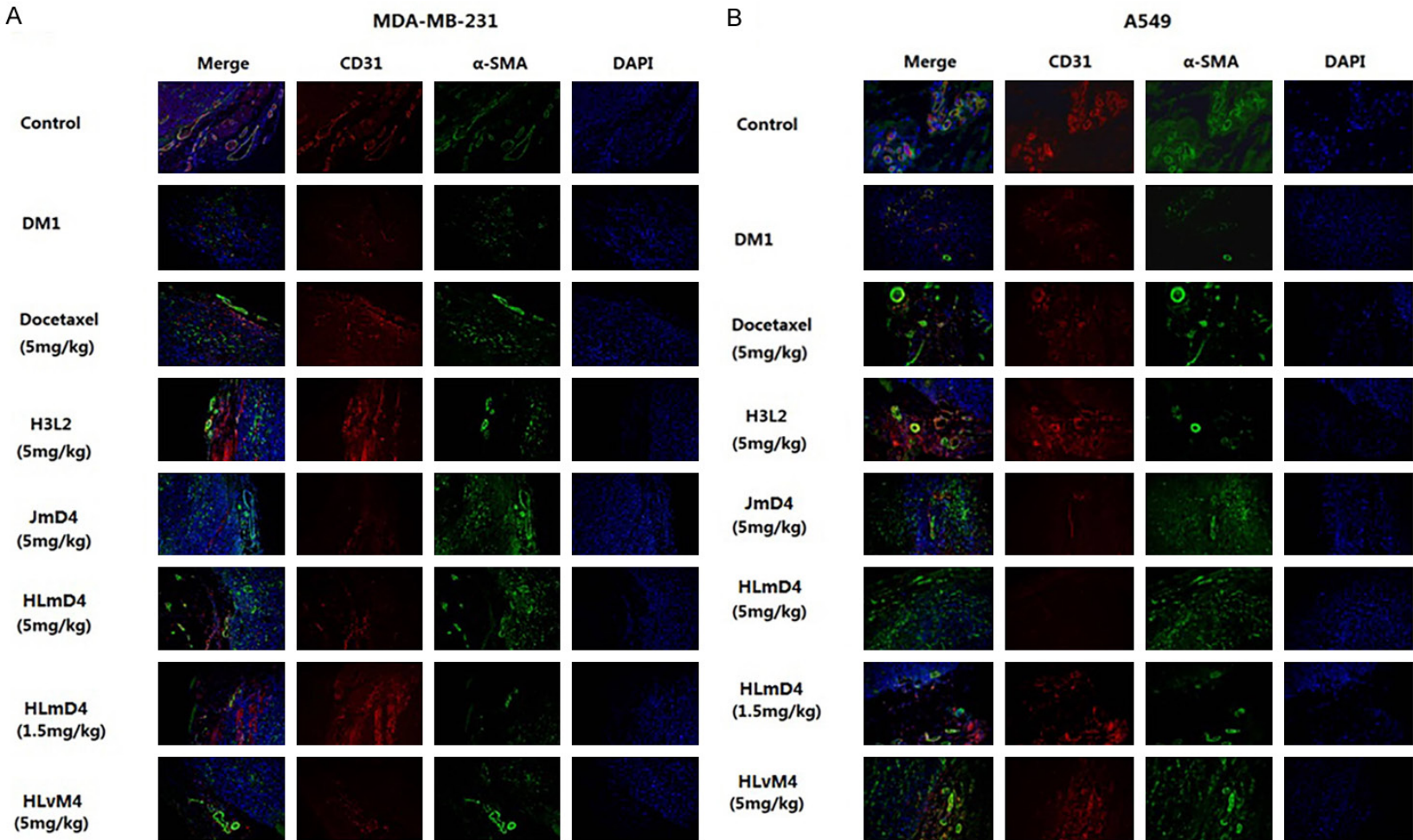


Figure 4. ADCs inhibits cell proliferation and induces apoptosis in MDA-MB-231 and A549 xenograft models. A, B. Tumour inhibition rates of different dosage groups (n = 6). 5 mg/kg HLmD4 resulted in significant tumour growth inhibition in both models. The arrows indicate dosing days except H3L2 group. C, D. IHC staining of Ki-67 (anti-Ki67 antibody) for proliferation in paraffin sections of xenografted tumours. Scale bar = 50 mm. E, F. IHC staining of cleaved-caspase 3 (anti-cleaved caspase 3) for apoptosis in paraffin sections of xenografted tumour. Scale bar = 50 mm. G, H. Quantifications of Ki67 or cleaved caspase 3 positive cells per field. Data are given as the mean ± SD (n = 3). *P < 0.05, **P < 0.001, ***P < 0.0001. NS: no significance.

Engineered site-specific ADCs have potent therapeutic activity



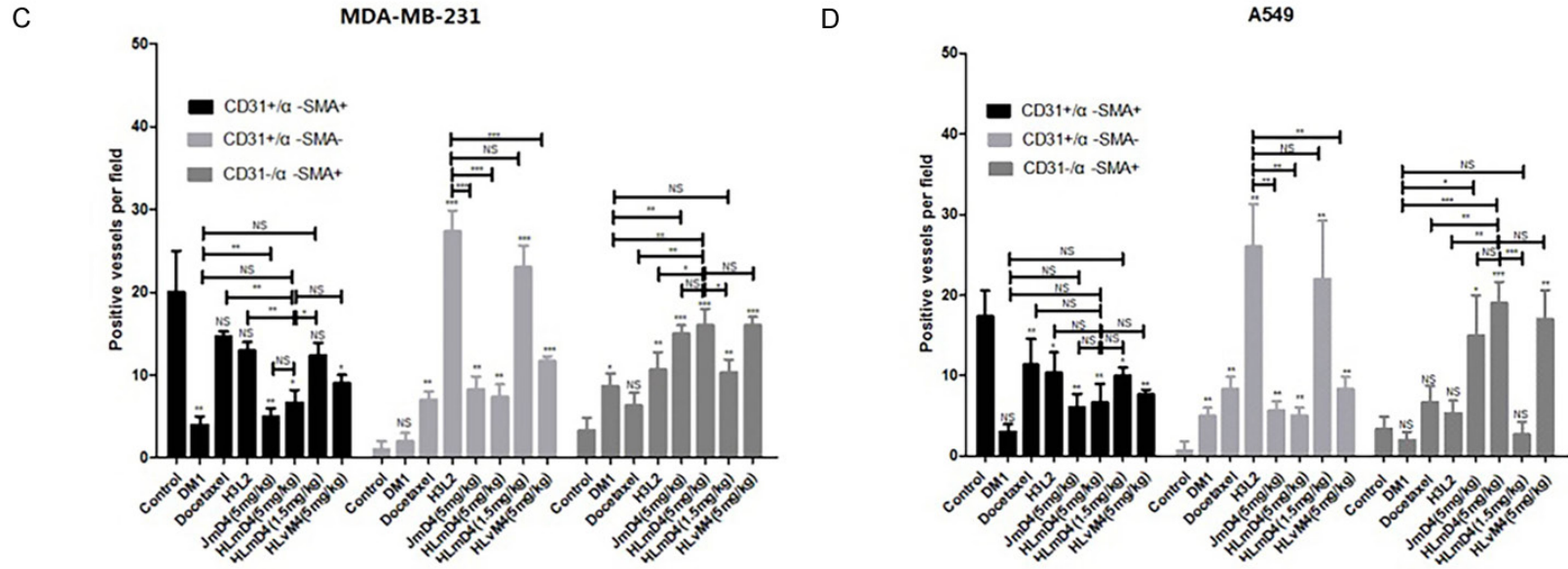
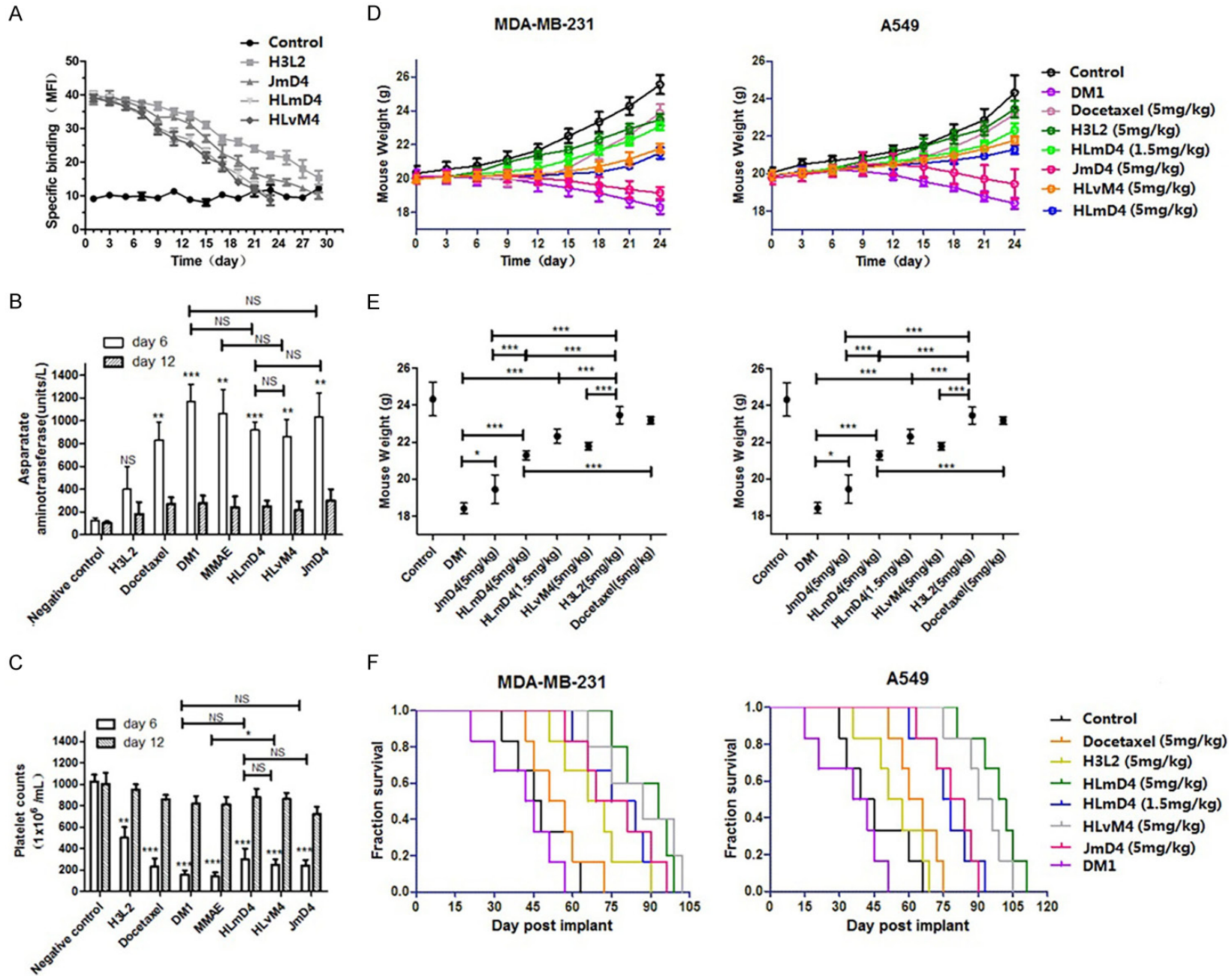


Figure 5. ADCs block angiogenesis and indirectly inhibit tumour growth in MDA-MB-231 and A549 tumours. A, B. Tumour vessel number and perfusion were determined by an antibody to SMA (green) for mural cells and a CD31 antibody (red) for vessel staining. Scale bar = 50 mm. C, D. Quantifications of mature (CD31+/α-SMA+) or immature (CD31+/α-SMA-) vessels per field. Data are given as the mean ± SD (n = 3). *P < 0.05, **P < 0.001, ***P < 0.0001. NS: no significance.

Engineered site-specific ADCs have potent therapeutic activity



Engineered site-specific ADCs have potent therapeutic activity

Figure 6. Engineered anti-DLL4 ADCs show lower toxicity than conventional ADC and small molecule drug in mouse safety studies. A. The plasma stability of ADCs was tested in BALB/c nude mouse (n = 6 animals/group, single i.v. dose on day 1). Changing values in blood over time relative to study day 1 were plotted. B, C. ICR mice (n = 5 animals/group, single i.v. dose on day 1) were given HLmD4, JmD4, HLvM4, H3L2, DM1 or Docetaxel at the indicated dose levels. Blood was drawn from mice on study days 6 and 12 for clinical chemistry (serum AST levels) and hematology (platelet counts). D, E. MDA-MB-231 or A549 xenograft BALB/c nude mouse models in different groups (n = 6) were weighed daily after dosing, and changes in body weight over time relative to study are plotted from day 1 to day 24. F. Survival rates of tumour-bearing mice in different groups (n = 6). In the MDA-MB-231 model and the A549 model, 5 mg/kg HLmD4 caused an effect to prolong evidently the length of survival. The arrows indicate dosing days except H3L2 group. Data are presented as the mean \pm SD, **P < 0.01, ***P < 0.0001. NS: no significance.

that toxicity of DM1 and JmD4 was significantly higher than that of the other drugs (**Figure 6D, 6E**). The reason why the tumour inhibition rate in the group treated with H3L2 was higher than that in the group treated with Docetaxel in the MDA-MB-231 model, and the result was opposite in the A549 model was that blocking the Notch pathway would inhibit MDA-MB-231 tumour growth, while blocking this pathway would promote A549 tumour proliferation [36, 37].

The survival rates of the tumour-bearing mice reflect the toxicity of the various tested drugs. In the MDA-MB-231 model, after the injection of the high dose of HLmD4 (or low dose), JmD4 and HLvM4, most mice (five of six) died within 93 (or 81) days, 74 days and 89 days. In the other mouse groups receiving H3L2, saline, Docetaxel and DM1, however, half of the animals survived for at least 70, 45, 55 and 45 days. After the treatment with the high dose of HLmD4 (or low dose), JmD4 and HLvM4 in the A549 model, five of six mice died, respectively, within 100 (or 79), 55 and 100 days. Furthermore, half of the animals treated with H3L2, saline, Docetaxel and DM1 survived for approximately 50, 40, 60 and 38 days. Notably, the engineered ADCs, HLmD4 and HLvM4, showed superior safety compared to traditional JmD4 in the two models. HLmD4 (5 mg/kg) dramatically prolonged the length of survival (**Figure 6F**).

According to the comparisons of the aspartate aminotransferase activity and platelet levels as well as the weight loss and the evolution of the survival rate of mice, the engineered ADCs, particularly HLmD4, appeared to have better antitumour activity than H3L2 and superior security than the conventional ADC and DM1 in both breast cancer and non-small lung cancer models. Moreover, the MDA-MB-231 model treated with drugs showed more potent selectivity and sensibility compared to the A549 model due to

the differences in the Notch signal mechanism in different tumour tissues.

Discussion

The aim of this study was to design engineered site-specific anti-DLL4 antibody conjugates (HLmD4 and HLvM4) and evaluate their antitumour activity and safety compared with the naked antibodies H3L2 and JmD4 prepared by traditional methods. We have recently shown that the humanized anti-DLL4 mAb, H3L2 mediated the antitumour effect by the inhibiting of tumour cell proliferation and promoting cell apoptosis in breast cancer xenograft tumours [30]. In the present work, we newly developed the ADCs HLmD4, JmD4 and HLvM4 and performed experiments. An ELISA was used to detect the affinities of the engineered and conventional ADCs (**Figure 2D**). Flow cytometry revealed that the conjugates were able to bind to HUVECs (**Figure 2B, 2C**). Then flow cytometry (**Figure 2E**) and Laser cofocal light microscopy (**Figure 2F, 2G**) were used to detect the internalization rates of these ADCs in DLL4-positive cells. Moreover, *in vitro* and *in vivo* plasma stability studies showed that the ADCs were stable for 144 h (**Figure 2H**). The results showed extremely similar characterizations of the ADCs compared with H3L2.

Since H3L2 and its variants are IgG1 antibodies, each antibody molecule contains four inter-chain disulphide bonds. We produced ADCs with engineered reactive cysteine residues using the THIOMAB™ technology developed by Genentech [38], which allows drugs to be conjugated with defined stoichiometry without disruption of the inter-chain disulphide bonds, including HLmD4, HmD2 and LmD2 (DAR = 3.96, 2.40 and 2.32, respectively), as analysed by HIC. Because it is generally accepted that the 4-DAR conjugate has a better preclinical effect than the 2-DAR conjugate, we selected the 4-DAR conjugate to research the antitu-

mour activity *in vitro* and *in vivo*. Moreover, we determined that HLmD4 had greater homogeneity than the non-site-specific JmD4 (**Figure 2A**). HLmD4 is as efficacious as JmD4 but has superior safety characteristics compared with JmD4 in the *in vivo* studies, especially with regard to liver toxicity, mouse weight assays and survival experiments (**Figure 6**).

Then, the ADCs, particularly the conjugates with DM1, successfully arrested the aggregation of α -tubulin and β -tubulin to inhibit tubulin and blocked cell growth in the G2/M phase of the cell cycle (**Figure 3C, 3F, 3G**). Thus, ADCs induced cell apoptosis and showed potent cell killing abilities *in vitro* in the MTT assay, caspase 3/7 activity test and apoptosis detection by FCS, which may be due to the differences in the toxicities of the ADCs (**Figure 3A, 3B, 3D, 3E**). In addition, HLmD4 exhibited potent anti-tumour activity in breast carcinoma and non-small cell lung xenograft tumour models through tumour inhibition rates, immunohistochemical staining and immunofluorescence assays (**Figures 4, 5**). Furthermore, compared with DM1, HLmD4 at a dose of 5 mg/kg exhibited a safer characterization, which invaded cells, including normal cells, due to the lack of targeting, in a survival-time experiment. And HLmD4 also induced a significantly durable regression of both xenografts, particularly in the MDA-MB-231 model. Based on various measurements and analyses, it is possible to conclude that the engineered HLmD4 displayed similar activity *in vitro* and equal efficacy *in vivo* at antibody doses comparable to the traditional JmD4, while the former had more advantages than the latter in safety research. Hence, anti-DLL4 ADCs can be selectively localized to the target and deliver high doses of drugs to breast tumour and lung cancer tissues.

However, the development of the new generation of ADCs still faces many challenges. Through the above introduction, we found that most ADCs under research or marketed are composed of small molecules and full-length antibodies, which typically represent nearly 95% of the mass of an ADC. Thus, usually, the distribution of ADCs into most tumour tissues is limited by the size of the antibody, which means that the antibody is possibly distributed into tumour tissue through the vasculature rather than being distributed into metabolizing

and eliminating organs, such as the intestines and liver, which potentially extends the half-life and limits systemic toxicity [39]. Recently, to improve tumour penetration, some studies have focused on antibody fragments because of their smaller size. Nevertheless, these fragments typically have a shorter half-life than the full-size antibodies. Therefore, both aspects need to be further studied in future work. On the other hand, although THIOmAB™ technology is very useful to improve the homogeneity of the final ADC product, we hope it is not the only way and more strategies should arise. Then, in 2017, the Scripps Research Institute (USA) developed Selenomab™ ADCs, which have one or more positioned selenocysteine residues that strategically permit fast and single step efficient reactions under near physiological conditions [40]. Moreover, there are other conjugation technologies based on alcohols and aldehydes, engineered aminoacyl-tRNA synthetases (aaRSs), oxidized sialic acids and transamination reagents [41, 42]. The emergence of these technologies is a good sign of targeted therapy. The next generation ADCs are increasingly being approved and entering pre-clinical and clinical trials because of the ongoing research aimed at improving efficacy and reducing side effects. A number of novel small-molecule families, engineered antibodies and new linker technologies are currently being researched, which provide hope for improved ADCs with the potential for improved safety and more effective cancer treatments.

In summary, we developed a unique, engineered, site-specific ADC targeting human DLL4, HLmD4, which is a highly potent and promising drug for the treatment of DLL4-positive breast cancer and non-small cell lung cancer malignancies, in safety and pharmacodynamic studies, providing a basis for further development of humanized anti-DLL4 ADC drugs for the treatment of DLL4-positive cancer diseases.

Acknowledgements

This work was supported by funds from the National Natural Science Foundation of China (NSFC81703404), a project funded by the Priority Academic Program Development of Jiangsu Higher Education Institutions (PAPD), Double First-Class University Project (CPU-2018GY14), a project fund by the Graduate

Engineered site-specific ADCs have potent therapeutic activity

Innovation Program of Jiangsu Province (SJK-Y19_0695) and College Students Innovation Project for the R&D of Novel Drugs.

Disclosure of conflict of interest

None.

Address correspondence to: Min Wu and Min Wang, State Key Laboratory of Natural Medicines, School of Life Science and Technology, China Pharmaceutical University, Nanjing 210009, China. E-mail: mickeywu2001@163.com (MW); minwang@cpu.edu.cn (MW)

References

- [1] Mailhos C, Modlich U, Lewis J, Harris A, Bicknell R and Ish-Horowicz D. Delta4, an endothelial specific notch ligand expressed at sites of physiological and tumor angiogenesis. *Differentiation* 2001; 69: 135-144.
- [2] Shutter JR, Scully S, Fan W, Richards WG, Kitajewski J, Deblandre GA, Kintner CR and Stark KL. Dll4, a novel notch ligand expressed in arterial endothelium. *Genes Dev* 2000; 14: 1313-1318.
- [3] Kuhnert F, Kirshner JR and Thurston G. Dll4-Notch signaling as a therapeutic target in tumor angiogenesis. *Vasc Cell* 2011; 3: 20.
- [4] Indraccolo S, Minuzzo S, Masiero M, Pusceddu I, Persano L, Moserle L, Reboldi A, Favaro E, Mecarozzi M, Di Mario G, Screpanti I, Ponzoni M, Doglioni C and Amadori A. Cross-talk between tumor and endothelial cells involving the notch3-Dll4 interaction marks escape from tumor dormancy. *Cancer Res* 2009; 69: 1314-1323.
- [5] Jubb AM, Soilleux EJ, Turley H, Steers G, Parker A, Low I, Blades J, Li JL, Allen P, Leek R, Noguera-Troise I, Gatter KC, Thurston G and Harris AL. Expression of vascular notch ligand delta-like 4 and inflammatory markers in breast cancer. *Am J Pathol* 2010; 176: 2019-2028.
- [6] Mullendore ME, Koorstra JB, Li YM, Offerhaus GJ, Fan X, Henderson CM, Matsui W, Eberhart CG, Maitra A and Feldmann G. Ligand-dependent Notch signaling is involved in tumor initiation and tumor maintenance in pancreatic cancer. *Clin Cancer Res* 2009; 15: 2291-2301.
- [7] You WK, Lee D, Choi Y and Kang KJ. Abstract LB-97: a novel anticancer bispecific antibody targeting VEGF and Dll4 inhibits tumor progression in lung and gastric cancer xenograft model. *Cancer Res* 2014; 74: LB-97.
- [8] Chiorean EG, LoRusso P, Strother RM, Diamond JR, Younger A, Messersmith WA, Adriaens L, Liu L, Kao RJ, DiCioccio AT, Kostic A, Leek R, Harris A and Jimeno A. A phase I first-in-human study of enoticumab (REGN421), a fully human delta-like ligand 4 (Dll4) monoclonal antibody in patients with advanced solid tumors. *Clin Cancer Res* 2015; 12: 2695-2703.
- [9] Pysz I, Jackson PJM and Thurston DE. Chapter 1: introduction to antibody-drug conjugates (ADCs). 2019.
- [10] Norsworthy KJ, Ko CW, Lee JE, Liu J, John CS, Przepiorka D, Farrell AT and Pazdur R. FDA approval summary: mylotarg for treatment of patients with relapsed or refractory CD33-positive acute myeloid leukemia. *Oncologist* 2018; 9: 1103-1108.
- [11] Shen Y, Yang T, Cao X, Zhang Y, Zhao L, Li H, Zhao T, Xu J, Zhang H, Guo Q, Cai J, Gao B, Yu H, Yin S, Song R, Wu J, Guan L, Wu G, Jin L, Su Y and Liu Y. Conjugation of DM1 to anti-CD30 antibody has potential antitumor activity in CD30-positive hematological malignancies with lower systemic toxicity. *MABs* 2019; 11: 1149-1161.
- [12] Menderes G, Bonazzoli E, Bellone S, Altwerger G, Black JD, Dugan K, Pettinella F, Masserdotti A, Riccio F, Bianchi A, Zammataro L, de Haydu C, Buza N, Hui P, Wong S, Huang GS, Litkouhi B, Ratner E, Silasi DA, Azodi M, Schwartz PE and Santin AD. Superior, in vitro, and, in vivo, activity of trastuzumab-emtansine (T-DM1) in comparison to trastuzumab, pertuzumab and their combination in epithelial ovarian carcinoma with high HER2/neu expression. *Gynecol Oncol* 2017; 1: 145-152.
- [13] Yurkiewicz IR, Muffly L and Liedtke M. Inotuzumab ozogamicin: a CD22 mAb-drug conjugate for adult relapsed or refractory B-cell precursor acute lymphoblastic leukemia. *Drug Des Devel Ther* 2018; 12: 2293-2300.
- [14] Dhillion S. Moxetumomab pasudotox: first global approval. *Drugs* 2018; 16: 1763-1761.
- [15] Syed YY. Tagraxofusp: first global approval. *Drugs* 2019; 5: 579-583.
- [16] Deeks ED. Polatuzumab vedotin: first global approval. *Drugs* 2019; 7: 1467-1475.
- [17] Challita-Eid PM, Satpayev D, Yang P, An Z, Morrison K, Shostak Y, Raitano A, Nadell R, Liu W, Lortie DR, Capo L, Verlinsky A, Leavitt M, Malik F, Aviña H, Guevara CI, Dinh N, Karki S, Anand BS, Pereira DS, Joseph IB, Doñate F, Morrison K and Stover DR. Enfortumab vedotin antibody-drug conjugate targeting nectin-4 is a highly potent therapeutic agent in multiple pre-clinical cancer models. *Cancer Res* 2016; 10: 1313.
- [18] Doi T, Shitara K, Naito Y, Shimomura A, Fujiwara Y, Yonemori K, Shimizu C, Shimoi T, Kuboki Y, Matsubara N, Kitano A, Jikoh T, Lee C, Fu-

Engineered site-specific ADCs have potent therapeutic activity

- jisaki Y, Ogitani Y, Yver A and Tamura K. Safety, pharmacokinetics, and antitumour activity of trastuzumab deruxtecan (DS-8201), a HER2-targeting antibody-drug conjugate, in patients with advanced breast and gastric or gastro-oesophageal tumours: a phase 1 dose-escalation study. *Lancet Oncol* 2017; 11: 1512-1522.
- [19] Francisco JA, Cerveny CG, Meyer DL, Mixan BJ, Klussman K, Chace DF, Rejniak SX, Gordon KA, DeBlanc R, Toki BE, Law CL, Doronina SO, Siegall CB, Senter PD and Wahl AF. cAC10-vc-MMAE, an anti-CD30-monomethyl auristatin E conjugate with potent and selective antitumor activity. *Blood* 2003; 102: 1458-1465.
- [20] Alley SC, Okeley NM and Senter PD. Antibody-drug conjugates: targeted drug delivery for cancer. *Curr Opin Chem Biol* 2010; 14: 529-537.
- [21] Pasut G and Veronese FM. Polymer-drug conjugation, recent achievements and general strategies. *Prog Polym Sci* 2007; 32: 933-961.
- [22] Junutula JR, Flagella KM, Graham RA, Parsons KL, Ha E, Raab H, Bhakta S, Nguyen T, Dugger DL, Li G, Mai E, Lewis Phillips GD, Hiraragi H, Fuji RN, Tibbitts J, Vandlen R, Spencer SD, Scheller RH, Polakis P and Sliwkowski MX. Engineered thio-trastuzumab-DM1 conjugate with an improved therapeutic index to target human epidermal growth factor receptor 2-positive breast cancer. *Clin Cancer Res* 2010; 19: 4769-4778.
- [23] Jaracz S, Chen J, Kuznetsova LV and Ojima I. Recent advances in tumor-targeting anticancer drug conjugates. *Bioorg Med Chem* 2005; 13: 5043-5054.
- [24] Yao X, Jiang J, Wang X, Huang C, Li D, Xie K, Xu Q, Li H, Li Z, Lou L and Fang J. A novel humanized antiHER2 antibody conjugated with MMAE exerts potent anti-tumor activity. *Breast Cancer Res Treat* 2015; 153: 123-133.
- [25] Remillard S, Rebhun LI, Howie GA and Kupchan SM. Antimitotic activity of the potent tumor inhibitor maytansine. *Science* 1975; 189: 1002-1005.
- [26] Huang AB, Lin CM and Hamel E. Maytansine inhibits nucleotide binding at the exchangeable site of tubulin. *Biochem Biophys Res Commun* 1985; 128: 1239-1246.
- [27] Mullard A. Maturing antibody-drug conjugate pipeline hits 30. *Nat Rev Drug Discov* 2013; 12: 329-332.
- [28] Verma S, Miles D, Gianni L, Krop IE, Welslau M, Baselga J, Pegram M, Oh DY, Diéras V, Guardino E, Fang L, Lu MW, Olsen S and Blackwell K; EMILIA Study Group. Trastuzumab emtansine for HER2-positive advanced breast cancer. *N Engl J Med* 2013; 368: 1783-1791.
- [29] Wang S, Zhou R, Sun F, Li R, Wang M and Wu M. The two novel DLL4-targeting antibody-drug conjugates MvM03 and MGD03 show potent anti-tumour activity in breast cancer xenograft models. *Cancer Lett* 2017; 409: 125-136.
- [30] Jia X, Wang W, Xu Z, Wang S, Wang T, Wang M and Wu M. A humanized anti-DLL4 antibody promotes dysfunctional angiogenesis and inhibits breast tumor growth. *Sci Rep* 2016; 6: 27985.
- [31] Xu Z, Wang Z, Jia X, Wang L, Chen Z, Wang S, Wang M, Zhang J and Wu M. MMGZ01, an anti-DLL4 monoclonal antibody, promotes nonfunctional vessels and inhibits breast tumor growth. *Cancer Lett* 2015; 372: 118-127.
- [32] Ding L, Tian C, Feng S, Fida G, Zhang C, Ma Y, Ai G, Achilefu S and Gu Y. Small sized EGFR1 and HER2 specific bifunctional antibody for targeted cancer therapy. *Theranostics* 2015; 5: 378-398.
- [33] Shen BQ, Xu K, Liu L, Raab H, Bhakta S, Kenrick M, Parsons-Reponte KL, Tien J, Yu SF, Mai E, Li D, Tibbitts J, Baudys J, Saad OM, Scales SJ, McDonald PJ, Hass PE, Eigenbrot C, Nguyen T, Solis WA, Fuji RN, Flagella KM, Patel D, Spencer SD, Khawli LA, Ebens A, Wong WL, Vandlen R, Kaur S, Sliwkowski MX, Scheller RH, Polakis P and Junutula JR. Conjugation site modulates the in vivo stability and therapeutic activity of antibody-drug conjugates. *Nat Biotechnol* 2012; 30: 184-189.
- [34] Luscan R, Mechaussier S, Paul A, Tian G, Gérard X, Defoort-Dellhemmes S, Loundon N, Audo I, Bonnin S, LeGargasson JF, Dumont J, Goudin N, Garfa-Traoré M, Bras M, Pouliet A, Bessières B, Boddaert N, Sahel JA, Lyonnet S, Kaplan J, Cowan NJ, Rozet JM, Marlin S and Perrault I. Mutations in TUBB4B cause a distinctive sensorineural disease. *Am J Hum Genet* 2017; 101: 1006-1012.
- [35] Saleem M, Asif J, Asif M and Saleem U. Amygdalin, from apricot kernels, induces apoptosis and causes cell cycle arrest in cancer cells: an updated review. *Anticancer Agents Med Chem* 2018; 18: 1650-1655.
- [36] Yang YL, Jablons D and You L. An alternative way to initiate Notch1 signaling in non-small cell lung cancer. *Transl Lung Cancer Res* 2014; 3: 238-241.
- [37] Osanyingbemi-Obidi JO, et al. Abstract 5209: the roles of Notch signaling in the development of non-small cell lung cancer. *Cancer Res* 2011; 71: 5209-5209.
- [38] Junutula JR, Raab H, Clark S, Bhakta S, Leipold DD, Weir S, Chen Y, Simpson M, Tsai SP, Dennis MS, Lu Y, Meng YG, Ng C, Yang J, Lee CC, Duenas E, Gorrell J, Katta V, Kim A, McDorman K, Flagella K, Venook R, Ross S, Spencer SD, Lee Wong W, Lowman HB, Vandlen R, Sliwkowski MX, Scheller RH, Polakis P and Mallet W. Site-specific conjugation of a cytotoxic drug to an antibody improves the therapeutic index. *Nat Biotechnol* 2008; 26: 925.

Engineered site-specific ADCs have potent therapeutic activity

- [39] Peters C and Brown S. Antibody-drug conjugates as novel anti-cancer chemotherapeutics. *Biosci Rep* 2015; 35: e00225.
- [40] Li X, Nelson CG, Nair RR, Hazlehurst L, Moroni T, Martinez-Acedo P, Nanna AR, Hymel D, Burke TR Jr and Rader C. Stable and potent selenomab-drug conjugates. *Cell Chem Biol* 2017; 24: 433-442.
- [41] Cahuzac B, Berthonneau E, Birlirakis N, Guittet E and Mirande M. A recurrent RNA-binding domain is appended to eukaryotic aminoacyl-tRNA synthetases. *EMBO J* 2000; 19: 445-452.
- [42] Ohashi K, Sada KE, Nakai Y, Matsushima S, Asano Y, Hayashi K, Yamamura Y, Hiramatsu S, Miyawaki Y, Morishita M, Katsuyama T, Katsuyama E, Watanabe H, Tatebe N, Narazaki M, Matsumoto Y, Sunahori Watanabe K, Kawabata T and Wada J. Cluster analysis using anti-aminoacyl-trna synthetases and SS-A/Ro52 antibodies in patients with polymyositis/dermatomyositis. *J Clin Rheumatol* 2019; 25: 246-251.